Study of Strontium Titanate and Barium Zirconate Properties Using Molecular Dynamics Simulation

by

Goh Wen Fong

Thesis submitted in fulfillment

of the requirements for the degree of

Master of Science

May 2013

"Imagination is more important than knowledge. For knowledge is limited, whereas imagination embraces the entire world, stimulating progress, giving birth to evolution."

Albert Einstein

Acknowledgements

I would like to express my gratitude to all the people who helped me in this research. This work could not have been accomplished without the help of these people.

First, I would like to thank Assoc. Prof. Dr. Sohail Aziz Khan for his useful advice and suggestions during the progress of the study. The papers could not have been published without his help. His advice and contribution towards successful completion of this work are highly appreciated.

Second, I am grateful to Dr. Yoon Tiem Leong for providing me a pleasant and tranquil workplace, in which I regarded as one of the most important factors to succeed.

Third, I would like to thank my family and my friends for their constant supports and understandings. Special thanks goes to Ms. Ching Chin Peng, for her help, support, motivation and encouragement throughout the study.

Lastly, I would like to acknowledge the support from the USM Fellowship.

Contents

List of Tables

List of Figures

Abbreviations

$BaZrO_3$	**B**arium **Z**irconate
$SrTiO_3$	**S**trontium **T**itanate
MD	**M**olecular **D**ynamics
NEMD	**N**on-**E**quilibrium **M**olecular **D**ynamics
SC	**S**imple **C**ubic
BCC	**B**ody-**C**entered **C**ubic
FCC	**F**ace-**C**entered **C**ubic
DNA	**D**eoxyribo**N**ucleic **A**cid

Physical Constants

Boltzmann Constant	k_B	=	$1.3806503 \times 10^{-23}$ m^2 kg s^{-2} K^{-1}
Gas Constant	R	=	8.314472 J mol^{-1} K^{-1}
Planck Constant	$\hbar$	=	1.054572×10^{-34} m^2 kg s^{-1}
Coulomb Constant	k_e	=	8.987552×10^{9} N m^2 C^{-2}
Avogadro constant	N_A	=	6.022142×10^{23} mol^{-1}
Force Constant	f_0	=	1.0 kcal Å^{-1} mol^{-1}

Symbols

r	interatomic seperation	Å
q	coulomb charge	e
σ	ionic radii	Å
ρ	ionic softness	Å
C	Van der Waals attraction parameter	kcal$^{\frac{1}{2}}$ Å^3 mol$^{-\frac{1}{2}}$
D	potential well depth	kcal mol^{-1}
Ω	potential steepness	Å^{-1}
r_0	equilibrium distance	Å
δt	time step	s
r_c	cut-off distance	Å
T	temperature	K
P	pressure	Pa or atm
E	total energy	kcal (1 kcal = 4184 J)
K	kinetic energy	kcal
U	potential energy	kcal
H	enthalpy	kcal
t	time	s
J	heat flux	W m^{-2}
L	length of simulation cell	Å or unit cell

a	lattice constant	Å
b	lattice constant	Å
c	lattice constant	Å
A	angle	° (deg)
B	angle	° (deg)
Γ	angle	° (deg)
ϱ	density	kg m^{-3}
V	molar volume	m^3 mol^{-1}
α	linear thermal expansion coefficient	K^{-1}
β_T	isothermal compressibility	Pa^{-1}
C_P	heat capacity at constant pressure	J mol^{-1} K^{-1}
κ	thermal conductivity	W m^{-1} K^{-1}

KAJIAN TENTANG STRONTIUM TITANAT DAN BARIUM ZIRCONAT DENGAN MENGGUNAKAN SIMULASI DINAMIK MOLEKUL

ABSTRAK

Simulasi dinamik molekul telah dijalankan ke atas bahan-bahan perovskit strontium titanat dan barium zirkonat dalam usaha untuk mengkaji tingkahlaku atom mikroskopik, dan termodinamik makroskopik serta sifat-sifat pengangkutan haba mereka. Keupayaan rumit atom boleh dipermudahkan kepada interaksi berpasangan yang terdiri daripada interaksi ionik, tolakan jarak dekat, tarikan Van der Waals dan ikatan kovalen Morse. Set parameter-parameter keupayaan strontium titanat dan barium zirkonat yang baru telah diperolehi. Fungsi penaburan jejarian telah diperolehi untuk mengkaji tingkahlaku atomik dan strukturnya. Parameter-parameter struktur, pekali pengembangan terma, kebolehmampatan sesuhu, kapasiti haba dan konduktiviti haba telah dinilai dalam lingkungan suhu 298 - 2000 K dan tekanan daripada 1 atm kepada 20.3 GPa. Pada suhu bilik, nilai-nilai parameter kekisi strontium titanat and barium zirkonat adalah 3.9051 Å dan 4.1916 Å. Pengiraan pekali pengembangan haba strontium titanat and barium zirkonat memberi nilai 1.010 $\times 10^{-5}\mathrm{K}^{-1}$ dan 0.816 $\times 10^{-5}\mathrm{K}^{-1}$ pada 298 K, manakala pengiraan kebolehmampatan sesuhu memberi nilai 5.800 $\times 10^{-12}\mathrm{Pa}^{-1}$ kepada strontium titanat dan 7.338 $\times$ 10^{-12} Pa^{-1} kepada barium zirkonat. Kapasiti haba strontium titanat and barium zirkonat adalah 126.8 J mol^{-1} K^{-1}

dan 110.8 J mol^{-1} K^{-1} pada suhu bilik. Pengiraan kekonduksian terma telah dilakukan dengan menggunakan kaedah dinamik molekul tak-seimbang, dan pembetulan kepada kesan saiz telah dilakukan. Peda suhu bilik, nilai-nilai konduktiviti haba strontium titanat and barium zirkonat adalah 11.04 W m^{-1} K^{-1} dan 4.263 W m^{-1} K^{-1}. Keputusan-keputusan simulasi memperlihatkan persetujuan yang baik dengan penemuan-penemuan eksperimen.

STUDY OF STRONTIUM TITANATE AND BARIUM ZIRCONATE PROPERTIES USING MOLECULAR DYNAMICS SIMULATION

ABSTRACT

Molecular dynamics simulation has been carried out on strontium titanate and barium zirconate in order to study the microscopic atomic behavior, and the macroscopic thermodynamic and thermal transport properties of the perovskite materials. The intricate interatomic potentials can be simplified into pairwise interactions, which consist of ionic interaction, short-range repulsion, Van der Waals attraction and Morse covalent bonding. New sets of potential parameters of strontium titanate and barium zirconate have been presented. Radial distribution functions have been obtained to study the atomic and structural behavior. Structural parameters, thermal expansion coefficient, isothermal compressibility, heat capacity and thermal conductivity have been evaluated in the temperature range of 298 - 2000 K and pressure ranging from 1 atm to 20.3 GPa. At room temperature, the values of lattice parameters of strontium titanate and barium zirconate are obtained to be 3.9051 Å and 4.1916 Å. While the calculation of thermal expansion coefficients of strontium titanate and barium zirconate gives 1.010 $\times 10^{-5} K^{-1}$ and 0.816 $\times 10^{-5} K^{-1}$ at 298 K, the isothermal compressibility of the materials yields 5.800 $\times 10^{-12} Pa^{-1}$ for strontium titanate and 7.338 $\times$ 10^{-12} Pa^{-1} for barium zirconate. The heat capacity of strontium titanate and barium zirconate are calculated to be 126.8 J mol^{-1} K^{-1} and 110.8 J mol^{-1} K^{-1} at

room temperature. Thermal conductivity calculation was performed using non-equilibrium molecular dynamics method, and correction for finite size effects has been made. At room temperature, the values of thermal conductivities are obtained to be 11.04 W m^{-1} K^{-1} for strontium titanate and 4.263 W m^{-1} K^{-1} for barium zirconate. The simulation results show good agreement with the experimental findings.

Chapter 1

Introduction

For development of technology and to meet new demands of tomorrow's society, there is a constant need for new materials with new or improved properties. Compounds with perovskite structure have shown many intriguing properties, such as ferroelectricity, high temperature superconductivity, high dielectric constant, piezoelectricity, thermoelectricity, etc. These properties make the perovskite compounds a suitable functional materials for applications in many areas. For example, barium titanate $BaTiO_3$ can be used to produce ferroelectric memories in constrast to the conventional dielectric memories, and lead zirconate titanate $Pb(Zr_xTi_{1-x})O_3$ $(0 \leq x \leq 1)$ or simply PZT can be used to manufacture piezoelectric transducers. Therefore these materials will continue to attract great interest. Despite the fact that there are tons of perovskite materials that show interesting properties and useful applications, particular interest has been given to strontium titanate $SrTiO_3$ and barium zirconate $BaZrO_3$ ceramic materials in this study.

$SrTiO_3$, which is one of the most common ceramic materials, possesses an ideal cubic perovskite structure with lattice constant of 3.9051 Å [2] and space group of

$Pm\bar{3}m$ at room temperature. Below 105 K, it is in a ferroelectric phase [3]. This perovskite material finds useful applications, among other things, in electronics and electrical insulations. Furthermore, it has been shown by some researchers that its electrical, thermal and thermoelectric properties can be greatly modified by introducing oxide defects or doped with alkaline earth metals or transition metals. For instance, niobium-doped strontium titanate can be electrically conductive [4], lanthanum-doped strontium titanate is a promising thermoelectric material [5, 6] and cerium-doped strontium titanate can be used in fuel cells applications [7].

On the other hand, $BaZrO_3$, which has a cubic perovskite structure with lattice constant of 4.192 Å [8] and space group of $Pm\bar{3}m$ at room temperature, is one of the most useful ceramic materials. Since it is stable with the paraelectric cubic structure, it does not show phase transition with temperature [9]. This perovskite material has a wide range of applications, including thermal barrier coating [10], nuclear fuel [11], refractory [12] and protonic ceramic fuel cell [13].

Since some of the devices made from these materials operate at high temperature and high pressure, it is important to understand the physical properties and stabilities of the materials at these extreme conditions. However, performing experiments at these extreme conditions can be costly or difficult or even impossible due to practical limitations. Conversely, computer simulations provide an alternative route to evaluate the materials' physical properties at these extreme cases. Computer simulations are not only useful to investigate the materials' macroscopic behavior, they are also powerful to study materials from the microscopic point of view, such as obtaining the atomic structure, which is usually done by using x-ray diffraction method.

Molecular dynamics simulation, which belongs to one of the two main families of computer simulations (the other one is Monte Carlo simulation), has been a promising tool for study of various kind of materials, from simple crystalline structures, such as solid argon [14], to complex bio-molecular structures, such as proteins [15] and DNA [16]. Just to mention some, molecular dynamics method has been used to study thermal-physical properties of alkali nitrate salts [17], rare-earth zirconates [18], magnesium silicate $MgSiO_3$ perovskite [19, 20], $Bi_{2.5}Na_{1.5}Nb_3O_{12}$ compounds [21], neptunium dioxide NpO_2 [22], uranium dioxide UO_2 [23] and carbon nanotubes [24, 25]. The potentials used in molecular dynamics simulations have also been formulated from a simple Lennard-Jones pairwise potential into much involved potentials, such as embedded-atom method (EAM) potentials for metals and metal alloys [26, 27], reactive force-field for hydrocarbons [28], three-body potential [29, 30], etc. Furthermore, the techniques have also been improved to couple with genetic algorithm [31, 32] and ab-initio method [33].

In this study, molecular dynamics simulations have been carried out to understand the thermodynamic and thermal transport properties of $SrTiO_3$ and $BaZrO_3$ perovskite materials in the temperature range of $298 - 2000$ K and pressure range from 1 atm to 20.3 GPa. Due to the fact that some of the potential parameters found in the literature cannot reproduce some of the properties, new and more accurate sets of potential parameters of $SrTiO_3$ and $BaZrO_3$ have been derived. Using our own derived potential parameters, we would like to explore the possibility of obtaining the structural parameters, thermal expansion coefficient, isothermal compressibility, heat capacity and thermal conductivity of the compounds. Furthermore, using molecular dynamics simulations, we hope to

enhance our understanding on the perovskite materials not only from the macroscopic point of view, but also the physics behind the macroscopic properties. In addition, we would like to obtain the relation between the atomic behavior and the observed macroscopic properties. In order to obtain good predictions of the macroscopic physical properties, one of the criteria is that the interatomic interactions must be described correctly. Correctness of the simulation results can be gauged by comparing against the experimental data. Moreover, it is hoped that this study could serve as a reference to researchers using molecular dynamics simulation to perform similar calculations on other materials.

In summary, the aim of this research is to:

- Derive more accurate sets of potential parameters of strontium titanate and barium zirconate.
- Obtain the variations of structural parameters, thermal expansion coefficient, isothermal compressibility, heat capacity and thermal conductivity of the perovskites with temperature and pressure.
- Study the radial distribution functions of the materials.
- Compare the simulation results against the experimental findings.

The thesis is organized is such a way that after theories of solid state physics and molecular dynamics are introduced, methodology of the research is described and follow by results and discussions. Lastly, conclusions are made and some recommendations for futher study are proposed.

Chapter 2

Background Theory I - Solid State Physics

Solid state physics, which is the largest branch of condensed matter physics, is one of the fundamental studies in physics. It is a study that covers every aspects related to crystalline materials, or rather, it is a study of macroscopic properties of crystalline materials which results from their constituent microscopic bahavior. Since the invention of the transistor, where smaller and lighter electronic devices are made possible, solid state physics has become a very important field of study. For example, the computers in the past were as huge as a room, but nowadays, the computers are much smaller that they are able to be fit into a workspace, or even carry along, at the same time, their performances have been improved tremendously. These innovations have to be attributed to the intensive progresses made on both theoretical and experimental studies in solid state physics. Furthermore, due to the advent of the economical high speed computers, the theoretical studies on crystalline materials have made the research even more progressive.

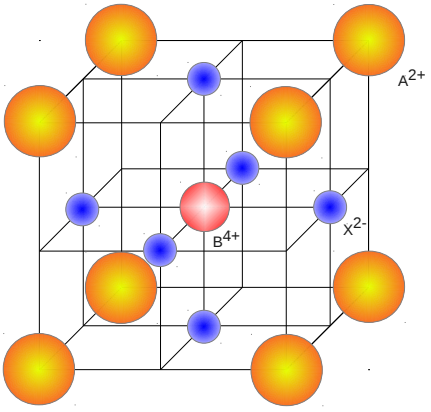

FIGURE 2.1: Conventional unit cell of a perovskite crystal.

2.1 Perovskite Structure

Perovskites are important in material science due to their interesting properties and useful applications in many areas.The physical properties of interest among perovskites include superconductivity, ferroelectricity, magnetic properties, electric conductivity, dielectric properties, etc. A lot of materials with perovskite structure have been discovered. Some of the compounds that possess perovskite structure are $CaTiO_3$, $BaTiO_3$, $SrTiO_3$, $CdTiO_3$, $PbTiO_3$, $SrZrO_3$, $BaZrO_3$, $KNbO_3$, $LiNbO_3$, $LiTaO_3$, $BaPrO_3$, $CsCaF_3$, $LiBaF_3$, and many more.

Perovskite structure, which has a very high symmetry, is a crystal structure with simple cubic lattice, as shown in Figure 2.1. The general chemical formula for perovskite compounds are ABX_3, where A and B are cations and X is an anion. A^{2+} and B^{4+} cations have different sizes, in which A^{2+} is larger than B^{4+}. A^{2+} ions are located at the corners of the cube, B^{4+} ions are located at the centers, and X^{2-} ions are located at the faces of the cube. Thus, there are five atoms in a conventional cell, and hence, five atoms per lattice point or five atoms in a primitive cell. X^{2-} anions are bonded to both A^{2+} and B^{4+}

cations. Each B^{4+} cation has six nearest neighbours, whereas each A^{2+} cation has twelve. Thus, B^{4+} and X^{2-} ions form octahedrons, while A^{2+} and X^{2-} ions form cuboctahedrons in the perovskite. The requirement of relative ionic sizes for stability of the perovskite is rigorous, so a slight distortion might cause the structure to reduce to a lower symmetry, in which the coordination numbers will be reduced.

2.2 Thermal Properties

One of our main interests in this work is to study thermal properties of materials. Therefore, it is important to understand how the expressions of the thermal properties are obtained. Hence, the derivations of heat capacity and thermal conductivity are shown here.

2.2.1 Derivations of Heat Capacities of Solids

Heat capacity is a measurable physical quantity that characterizes the amount of heat required to change the temperature of a substance of 1 kg by 1 K. In this section, the derivation of the specific heat from classical treatment is discussed.

Consider a solid system of N atoms held in their respective positions and are free to vibrate independently. In classical theory, the atoms are assumed to vibrate like classical harmonic oscillators. Thus, the atomic vibrations can be regarded as spring vibrations, which execute small vibrations about their equilibrium positions. The energies due to the motion of each atom along the three

directions are

$$E_x = \frac{p_x^2}{2m} + \frac{1}{2}kx^2 \tag{2.1}$$

$$E_y = \frac{p_y^2}{2m} + \frac{1}{2}ky^2 \tag{2.2}$$

$$E_z = \frac{p_z^2}{2m} + \frac{1}{2}kz^2 \tag{2.3}$$

where the spring constants k are taken to be the same along the three directions. If the temperature is sufficiently high, the atomic oscillators can be treated using classical statistical mechanics. At this point, it is useful to state the equipartition theorem (further discussion can be found in Section 3.4.3):

Equipartition Theorem

> For a system in thermal equilibrium at temperature T, a generalized position or momentum that occurs in the Hamiltonian only as a quadratic term contributes an energy of $\frac{1}{2}k_BT$ to the mean energy of the system, where k_B is the Boltzmann constant.

Thus, according to equipartition theorem, the mean energy of the solid of N atoms is

$$\begin{aligned} \bar{E} &= N(E_x + E_y + E_z) \\ &= 3N(\frac{1}{2}k_BT + \frac{1}{2}k_BT) \\ &= 3Nk_BT = 3RT \end{aligned} \tag{2.4}$$

where $R = 8.314$ J/Kmol is the gas constant. The specific heat of the solid is

$$\begin{aligned} C_V &= \left(\frac{\partial E}{\partial T}\right)_V \\ &= 3R = 24.94 \text{ J/Kmol} \end{aligned} \tag{2.5}$$

Some solids such as aluminium, copper and germanium, have specific heat values close to 24.94 J/Kmol. However, some substances such as diamond and silicon has a much lower specific heat value. This can be understood that the classical treatment is valid only when the temperature T is high enough so that $k_B T \gg \hbar\omega$, where $\hbar$ is the Planck constant and ω is the vibrational frequency. $C_V = 24.94$ J/Kmol is called the Dulong-Petit limit. Furthermore, note that Equation 2.5 does not depend on temperature. This is also incorrect as when the temperature goes to zero, the specific heat approaches zero as well. Thus, it can be concluded that the classical treatment only works fine at very high temperature. In order to obtain agreement at all temperatures, quantum mechanical treatment is required.

2.2.2 Derivation of Thermal Conductivity

If thermal conduction is viewed from a microscopic angle, the heat energy is transferred by the diffusion and collisions of particles, such as electrons, atoms, molecules and phonons within a body due to a temperature gradient. From a macroscopic point of view, a temperature gradient causes heat to flow from a region with higher temperature to a region with lower temperature. The heat flux, which is the heat energy crossing per unit area per unit time is expressed according to the Fourier's law of heat conduction:

$$J_x = -\kappa \frac{dT}{dx} \tag{2.6}$$

where dT/dx is the temperature gradient along the x direction and the coefficient κ is known as the thermal conductivity.

Imagine a slab in which the temperatures are varied. If only the x direction is considered, 1/6 of the particles will move toward the $+x$ direction, and similarly 1/6 of the particles will diffuse toward the $-x$ direction. Assume that the particles collisions happened at the middle of the slab along the x direction. If the mean free path of the particle collisions is let to be l, the last collisions of the particles which diffuse toward the $+x$ direction happen to be at position of $x - l$, whereas the last collisions of the counterparts take place at $x + l$. Therefore, the energies of the particles can be evaluated at these positions. Hence, the mean energy transported per unit area per unit time towards the $+x$ direction is

$$J_{+x} = \frac{1}{6} n\bar{v}\bar{E}(x - l) \tag{2.7}$$

and similarly, the mean energy transported per unit area per unit time towards the $-x$ direction is

$$J_{-x} = \frac{1}{6} n\bar{v}\bar{E}(x + l) \tag{2.8}$$

where n is the concentration of the particles, $\bar{v}$ is the mean velocity of the particles, and $\bar{E}(x + l)$ and $\bar{E}(x - l)$ are the mean energies of the particles at $x + l$ and $x - l$ respectively. Thus, the net energy flows per unit area per unit time or the net energy flux is

$$\begin{aligned} J_{net} &= J_{+x} - J_{-x} \\ &= \frac{1}{6} n\bar{v}[\bar{E}(x - l) - \bar{E}(x + l)] \\ &= \frac{1}{6} n\bar{v} \left\{ \left[\bar{E}(x) - l\frac{\partial \bar{E}}{\partial x}] - [\bar{E}(x) + l\frac{\partial \bar{E}}{\partial x} \right] \right\} \\ &= -\frac{1}{3} n\bar{v} l \frac{\partial \bar{E}}{\partial x} \end{aligned} \tag{2.9}$$

In terms of derivative of T, Equation 2.9 becomes

$$J_{net} = -\frac{1}{3} n\bar{v}l \frac{\partial \bar{E}}{\partial T} \frac{\partial T}{\partial x} \tag{2.10}$$

Since the heat capacity per unit volume of the particles is

$$C_V = n\frac{\partial \bar{E}}{\partial T} \tag{2.11}$$

Equation 2.10 becomes

$$J_{net} = -\frac{1}{3} C_V \bar{v}l \frac{\partial T}{\partial x} \tag{2.12}$$

Comparing between Equation 2.6 and Equation 2.12 yields

$$\kappa = \frac{1}{3} C_V \bar{v}l \tag{2.13}$$

Equation 2.13 has been used to calculate the thermal conductivity by phonons, where C_V is treated as the specific heat of phonons, $\bar{v}$ is taken to be the speed of sound and l is the phonon mean free path. Note that at high temperatures, where the temperatures are much higher than the Debye temperature ($T \gg \Theta_D$), C_V obeys the Dulong-Petit law and is temperature-independent. Therefore, the thermal conductivity should be expected to decline with increasing temperature in the high-temperature regime, and the rate of decline is generally given by

$$\kappa \propto \frac{1}{T^{\eta}} \tag{2.14}$$

where η is somewhere between 1 and 2.

Chapter 3

Background Theory II - Molecular Dynamics

Molecular dynamics (MD) simulation is one of the powerful computer simulation techniques in the sense that it not only allows prediction of material's properties at macroscopic level, it also helps to understand the basic physics behind the macroscopic bahavior.

In MD simulation, we provide a 'guess' for the interatomic interactions and obtain 'exact' predictions of bulk properties. The predictions are exact in the sense that they can be made as accurate as we like, subject to the limitation of computer budget.

Besides, MD simulations also act as a bridge between theory and experiment, i.e. a theory may be tested by performing simulation using the same model, on the other hand, simulations may be carried out on the computers which are difficult or impossible to be performed in the laboratories, for example, working at extremes of temperature and pressure. Ultimately, we would like to make direct

comparisons with the experimental measurements made on specific materials, in which a good model of molecular interactions is essential.

The basic idea of MD simulation is to simulate the motions and assemblies of the atoms and molecules[1]. In other words, MD simulation provides means to solve the equation of motions of the interacting particles. Once the information of the system at the atomic level is known, macroscopic physical quantities are revealed via statistical mechanics.

3.1 Equations of Motion

Consider a system of N interacting particles, such as atoms and molecules, the Lagrange equations of motion are:

$$\frac{dL}{dx_k} - \frac{d}{dt}\left(\frac{dL}{d\dot{x}_k}\right) = 0 \tag{3.1}$$

where $k = 1, 2, 3$, and x_i and $\dot{x}_i$ are the generalized coordinates and velocities respectively. L is the Lagrangian of the particle:

$$L(x, \dot{x}) = K(\dot{x}) - U(x) \tag{3.2}$$

where K and U are the kinetic and potential energies of the particle.

If a system of atoms in Cartesian coordinates r is considered, the quantitative account of the Newton's second law of motion gives:

$$F_i = m_i \ddot{r}_i \tag{3.3}$$

[1] We shall called them particles for simplicity.

where m_i is the mass of the i^{th} particle, and

$$F_i = -\nabla U(r_i) \tag{3.4}$$

is the force experienced by the i^{th} particle.[2] Thus, solving Equation 3.3, which required the knowledge of the potential energy (Equation 3.4), gives the positions and velocities of the particles.

3.2 Non-bonded Molecular Interactions

In order to solve the equations of motion, a preliminary step is to determine the potential energy of the atomic system. The molecular interactions can be decomposed into non-bonded interactions and bonding interactions. In this section, non-bonded interactions are focused and the discussion on molecular bonding can be found elsewhere [34]. The non-bonded potential energy of the system of N interacting particles is formulated as a sum over the interactions between the particles in the system:

$$U(r) = \sum_i u(r_i) + \sum_i \sum_{j>i} v(r_i, r_j) + \sum_i \sum_{j>i} \sum_{k>j>i} w(r_i, r_j, r_k) + \dots \tag{3.5}$$

where the summations sum over all distinct pairs without counting any pair twice. The first term $u(r_i)$ characterizes an externally applied potential field or the effect of the container walls. However, when periodic boundaries are concerned, this term is usually ignored. The second term $v(r_i, r_j)$ represents a two-body potential and the third term $w(r_i, r_j, r_k)$ typifies a three-body potential. In most cases, the potential energy of the system is usually simplified into two-body potential or

[2] These equations also apply to molecules, where F_i is the total force experienced by i^{th} molecule at its center of mass.

pairwise potential, $v(r_i, r_j) = v(r_{ij})$, where r_{ij} is the distance between the i^{th} and j^{th} particles. Some of the most commonly used pairwise potential functions[3] will be discussed.

3.2.1 Lennard-Jones Potential

Lennard-Jones potential, which is also known as $6-12$ potential, is one of the earliest and most commonly used potentials. It is associated with Van der Waals (weak) interaction or dipole $-$ dipole dispersion. The functional form is

$$U_{LJ}(r_{ij}) = 4\phi[(\frac{\chi}{r_{ij}})^{12} - (\frac{\chi}{r_{ij}})^{6}] \tag{3.6}$$

where ϕ and χ are constant parameters that set the energy and distance scales associated with the interactions. The first term or the term to the power of 12 contributes repulsive force and the second term or the term to the power of 6 contributes attractive force. This potential has been used in the early studies of liquid Argon. For Argon, the optimised parameters are $\phi/k_B = 119.8$ and $\chi = 3.405$Å.

3.2.2 Born-Mayer-Huggins Potential

Another type of potential which also describes Van der Waals interaction is the Born-Mayer-Huggins potential or exponential $-$ 6 potential:

$$U_{Born}(r_{ij}) = f_0(\rho_{ij}) \exp\left(\frac{\sigma_{ij} - r_{ij}}{\rho_{ij}}\right) - \frac{C_{ij}}{r_{ij}^6} + \frac{\zeta_{ij}}{r_{ij}^8} \tag{3.7}$$

[3]For connections among the pairwise potential functions, see [35, 36].

where σ_{ij} represents the sum of ionic radii of i^{th} and j^{th} ions, ρ_{ij} symbolies the sum of ionic softness of i^{th} and j^{th} ions, and C_{ij} and ζ_{ij} correspond to dipole − dipole dispersion and dipole − quadrupole dispersion parameters respectively. The first term represents the exponential repulsion at short-range, the second term corresponds to Van der Waals attraction and the third term represents dipole − quadrupole dispersion.

3.2.3 Coulombic Potential

If electrostatic charges are presents in the system, there will be ionic or Coulombic forces interacting the ions in such a way that like charges repel each other, whereas opposite charges attract. The magnitudes of the forces depend on the electrostatic charges, thus, we have Coulombic potential:

$$U_{Coulomb}(r_{ij}) = k_e \frac{q_i q_j}{r_{ij}} \tag{3.8}$$

where q_i and q_j are the electrostatic charges of i^{th} and j^{th} ions, and k_e is the Coulomb constant.

3.2.4 Morse Potential

When dealing with 'hard' bonds, such as covalent bonds, it is useful to employ Morse potential. Morse potential is an empircal potential that describe an asymmetric covalent bonding between two ions, and it also accounts for bond breaking. The functional form of Morse potential is

$$U_{Morse}(r_{ij}) = D_{ij}\{\exp[-2\Omega_{ij}(r_{ij} - r_{0ij})] - 2\exp[-\Omega_{ij}(r_{ij} - r_{0ij})]\} \tag{3.9}$$

where D_{ij} is the depth of the potential well, Ω_{ij} is the steepness of the potential and r_{0ij} is the equilibrium distance between the ions. Unlike harmonic bonding, Morse potential caters the anharmonicity of real bond, which is more harder to compress than pull it apart, and this anharmonicity also contributes to material's thermal expansion.

3.3 Molecular Dynamics Algorithms

The basic idea in MD simulation is to solve the equations of motion, i.e. Equation 3.3. For each particle, the equations of motion according to Euler method are

$$\frac{dr_i}{dt} = v_i \tag{3.10}$$

and

$$\frac{dv_i}{dt} = \frac{F_i}{m_i} = a_i \tag{3.11}$$

where v_i and a_i are the resultant velocity and acceleration of i_{th} particle. If we choose a value δt to be the size of every time step, the one step of the equations of motion are

$$r_i(t + \delta t) = r_i(t) + v_i(t + \delta t/2)\delta t \tag{3.12}$$

and

$$v_i(t + \delta t) = v_i(t) + a_i(t + \delta t/2)\delta t \tag{3.13}$$

With the knowledge of the potential energies of the particles, the forces or accelerations can be derived, and thus, the atomic positions and velocities can be obtained. However, in MD simulation, we are interested in computing the motion over a very large number of time steps, and it turns out that the numerical

errors associated with Euler method are too big to tolerate. When accuracy is concerned, it is necessary to employ other scheme for solving the equations of motion.

3.3.1 Verlet Algorithm

Verlet algorithm [37] has smaller numerical errors associated if compared with Euler method. In order to derived the Verlet algorithm, we take Taylor expansion about $r_i(t)$, which yields:

$$r_i(t+\delta t) = r_i(t) + \delta t\ v_i(t) + (1/2)\delta t^2 a_i(t) + \dots \tag{3.14}$$

$$r_i(t-\delta t) = r_i(t) - \delta t\ v_i(t) + (1/2)\delta t^2 a_i(t) - \dots \tag{3.15}$$

Summing up Equations 3.14 and 3.15 gives

$$r_i(t+\delta t) = 2r_i(t) - r_i(t-\delta t) + \delta t^2 a_i(t) \tag{3.16}$$

Equation 3.16 is the ordinary Verlet algorithm for trajectories. It is remarkable to note that knowing the advanced positions only required the positions at both present and previous step, and also the accelerations at present step. Furthermore, it does not require the knowledge of the velocities. Although velocities are not needed to compute the trajectories, they are useful for estimating the kinetic energy (and hence the total energy). Taking the difference between Equations 3.14 and 3.15 produces the formula for velocities

$$v_i(t) = \frac{r_i(t+\delta t) - r_i(t-\delta t)}{2\delta t} \tag{3.17}$$

Note that the errors per integration step associated with Verlet algorithm are of the order of δt^4 for Equation 3.16 and δt^2 for Equation 3.17.

3.3.2 Timesteps

It is important to choose a proper time step δt in MD simulation. The time step should be large enough so that the time averages can be close to the averages in a macroscopic experimental system, and conversely, it should be small enough so that the computational resource is enough to ensure that time averages can be evaluated over a sufficient number of times. A typical time step used to integrate the equations of motion numerically is about 10^{-15} s or 1 fs. Since $\sim 10^6$ integration steps are normally adopted for a reasonable computing time, the simulation is restricted to about 10^{-9} s or 1 ns.

3.3.3 Periodic Boundary Condition

In a real system, where the number of particles is significantly large ($\sim 10^{23}$), the collisions between the particles and the walls of the container are negligible, since the system behavior would be dominated by collisions between particles. However, in computer simulation, the number of particles is not significantly large due to the limitation of computational resouces. In other words, we are limited to a small system, which contains a relatively small number of particles ($\sim 10^3$). Hence, the collisions between the particles and the walls can be significant and non-negligible. For example, consider 1000 atoms arranged in a $10 \times 10 \times 10$ cube, nearly half the atoms are on the outer faces, and the collisions between these particles and the walls will have a large effect on the measured properties. Therefore, it is useful to implement a periodic boundary condition.

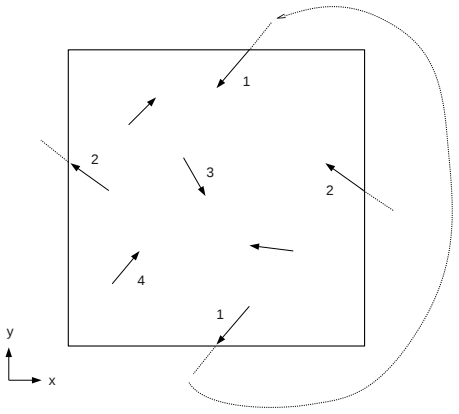

FIGURE 3.1: Schematic diagram of periodic boundary condition.

To understand periodic boundary condition, imagine that a particle is approaching a wall, and when the particle hits the wall, it is instantaneously transported to the opposite side of the wall and is like coming from that wall, as shown in Figure 3.1. By doing this, the collisions between the particles and the walls will be absolutely zero. It is important to bear in mind that even though the particle is transported to the opposite side, it can still affect the particle near the wall side because the particle can also be imagined to locate beyond the boundary. Thus, in order to calculate the particle interactions with periodic boundary condition imposed, the minimum image convention is adopted, in which the particles interact with the nearest particle or image in the periodic array. Therefore, this solve the boundary problem. However, special attention must be paid when considering properties which are influenced by long-range correlations, such as the imposed artificial heat flow in NEMD method.

3.3.4 Cut-off radius

In order to compute the particles' trajectories using Verlet algorithm, i.e. Equation 3.16, we have to, first of all, calculate the interatomic forces, which can be

obtained by computing the potential energies according to Equation 3.4. However, computing the non-bonded interatomic forces involved a great number of pairwise calculations if the potential energy has an infinite range, i.e. when considering each particle i, the force calculations are loop over all other particles j in order to obtain the atomic seperation r_{ij}. Since the potential energy becomes zero when the atomic seperation r_{ij} is very large, it is useful to implement a cut-off radius r_c and truncate the interatomic interactions when the interatomic seperation is greater than r_c. In other words, the force calculations are skipped if $r_{ij} > r_c$ and move on to consider other j particle. By this way, expensive calculations can be avoided and enormous computational resouces can be saved[4]. A typical cut-off radius r_c has a value of about 12 Å.

If cut-off radius is implemented, there will be a truncation in interatomic interactions. For example, when a particle crosses the cut-off radius, there will be a little 'jump' in the energy, and this creates a new problem as it will destroy the conservation of the energy. In order to correct for the energy, a tail correction is usually implemented. See [38] for more details.

3.3.5 Neighbour Lists

Although the force calculations can be skipped when the atomic seperation is greater than the cut-off radius, when examining the condition of $r_{ij} > r_c$ for all other particles j, this still consumes plenty of time. Verlet [37] suggested

[4]In order to understand this better, imagine that you have a mess of marbles on the floor but dispersed uniformly and you draw two circles with the their center overlapped and the radius of the second circle r_2 greater than that of the first one r_1, for instance $r_1 = 5$cm and $r_2 = 10$cm. If you count the number of marbles in the circles, you will find that the number of marbles in the circle with larger radius is not twice but is multiple times (about 4 times) of the number of marbles in the smaller circle, even though the radius of the second radius is twice as big as that of the fircle circle. In other words, calculation twice as big takes four times as long to complete. Thus, by skipping the calculations over the particles which are confined in the larger radius, great computing time can be saved.

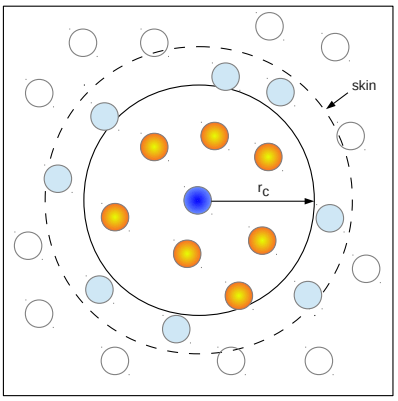

FIGURE 3.2: Schematic diagram of neighbour lists. Only pairs appearing in the list are checked in the force routine.

that construction of lists of nearby pairs of particles can be used to improve the speed of the program. To construct the so-called neighbour lists, each particle is surrounded by a 'skin', which has a radius slightly larger than the cut-off radius, and only particles that fall within the skin are listed as 'neighbours', as shown in Figure 3.2. Hence, each particle has a unique neighbour list. When the force calculations are carried out, only particles within the list are checked, and thus, this save a large amount of computing time, even though the lists need to be reconstructed from time to time. The choice of the skin radius, which is the distance between the skin and the cut-off radius, is a compromise, i.e. larger lists require less frequent update, but consume more computer time compared with smaller lists. So, the choice of skin radius need to be made by experimentation. A typical skin radius is about 2 Å.

3.4 Statistical Mechanics

In molecular dynamics simulation, we are not dealing with one or two particles, but we are dealing with a bunch of them. So, in order to understand the macroscopic behavior of a system with numerous particles, probabilities and statistics of the microscopic system have to be used to predict the macroscopic properties, which can be measured in the laboratory (like temperature, pressure, etc.). That's why statistical mechanics is important as it act as a bridge between atomic simulation and macroscopic properties, in which the properties of macroscopic bodies are predicted by the statistical behavior of their constituent microscopic parts. Therefore, with molecular dynamics simulation, which generate information at microscopic level, thermodynamic properties of the atomic system can be studied via statistical mechanics.

3.4.1 Ensembles

An ensemble is a collection of all possible systems which have an identical thermodynamic state but have different microscopic states.

In classical molecular dynamics, simulations are easily done in the microcanonical ensemble (NVE-constant), in which the number of particles, volume and energy are controlled. However, in real life, the temperature and/or pressure are controlled instead of the energy. In other words, the real-life physical properties are observed in canonical ensemble (NVT-constant) or isothermal-isobaric ensemble (NPT-constant). Thus, it is more useful to carry out the simulation in canonical ensemble or isothermal-isobaric ensemble, so that the simulated results are comparable to the experimental properties. Several popular methods that used to control the temperature in MD simulation are the velocity rescaling

method, Andersen thermostat, Nose-Hoover thermostat [39], Langevin thermostat [40], etc.

3.4.2 Time Average

In MD simulation, various physical quantities are monitored and their expectation values are determined by taking averages over the total configurations generated in the simulation or over the total time steps τ. Such averages are denoted as 'time average', although the word time does not necessarily mean physical time. For a physical quantity Q, the time average is

$$\bar{Q} = \frac{1}{\tau}\sum_{n=1}^{\tau} Q_n \tag{3.18}$$

If the size of the system is large enough and the simulation is long enough, these averages will be very close to the averages in a macroscopic experimental system, i.e. the ensemble averages, as according to the Ergodic hypothesis. Ensemble average is an average taken over many replicas of the system considered simultaneously. However, the system size and simulation time that can be achieved are limited, and hence, it might be useful to estimate the errors associated with the averaged quantities. The standard deviation ς associated with Equation 3.18 is

$$\varsigma = \sqrt{\bar{Q}^2 - \bar{Q}^2} \tag{3.19}$$

Note that equation 3.19 is a crude way to estimate the errors associated with the measured averaged quantities, because the data points generated from the simulation are usually not independent, conversely they are highly correlated since the configurations are usually stored sufficiently and frequently. Therefore,